Food & Function

ROYAL SOCIETY OF CHEMISTRY

PAPER

View Article Online
View Journal | View Issue

Cite this: *Food Funct.*, 2024, **15**, 4262

Stored white tea ameliorates DSS-induced ulcerative colitis in mice by modulating the composition of the gut microbiota and intestinal metabolites†

Zhiyuan Lin,‡[a,b] Weidong Dai,‡[a] Shanshan Hu,[b] Dan Chen,[a] Han Yan,[a] Liang Zeng *[b] and Zhi Lin *[a]

Received 24th November 2023,
Accepted 1st March 2024

DOI: 10.1039/d3fo05176e

rsc.li/food-function

Changes in the chemical composition of white tea during storage have been studied extensively; however, whether such chemical changes impact the efficacy of white tea in ameliorating colitis remains unclear. In this study, we compared the effects of new (2021 WP) and 10-year-old (2011 WP) white tea on 3% dextrose sodium sulfate (DSS)-induced ulcerative colitis in mice by gavaging mice with the extracts at 200 mg kg^{-1} day^{-1}. Chemical composition analysis showed that the levels of 50 compounds, such as flavanols, dimeric catechins, and amino acids, were significantly lower in the 2011 WP extract than in the 2021 WP extract, whereas the contents of 21 compounds, such as *N*-ethyl-2-pyrrolidinone-substituted flavan-3-ols, theobromine, and (−)-epigallocatechin-3-(3″-*O*-methyl) gallate, were significantly higher. Results of the animal experiments showed that 2011 WP ameliorated the pathological symptoms of colitis, which was superior to the activity of 2021 WP, and this effect was likely enhanced based on the decreasing of the relative abundance of the *g_bacteroides* and *g_Escherichia-Shigella* flora in mice with colitis and promoting the conversion of primary bile acids to secondary bile acids in the colon. These results will facilitate the development of novel functional products from white tea.

1. Introduction

Inflammatory bowel disease (IBD) is a chronic, idiopathic and complex inflammatory disease of the gastrointestinal tract that includes the two most general forms, ulcerative colitis (UC) and Crohn's disease (CD).[1] IBD has been classified as a refractory disease by the World Health Organization due to its long period of onset, patients' tendency to relapse, and susceptibility to deterioration in susceptible groups. The pathogenesis of IBD has not been fully elucidated, but it is generally thought to be related to dysregulation of the intestinal mucosal immune system, damage to the intestinal epithelial barrier, and dysbiosis of the gut microbiota.[2,3] The main therapeutic strategy has included anti-inflammatory drugs to modulate the immune system and inhibit mucosal immune responses and pro-inflammatory cytokine production; the utilized drugs include glucocorticoids, immunosuppressants, aminosalicylates, and biologics.[4] However, these treatments can lead to drug tolerance and adverse effects.[5,6] Therefore, there is an urgent need to find and investigate more effective and safer drugs for IBD treatment.

Tea is recognized as a healthy beverage, and recent studies have shown that tea has the potential to ameliorate and alleviate colitis.[7,8] This effect is mainly attributed to the high abundance of a variety of active ingredients, such as catechins, alkaloids, amino acids, and phenolic acids. These active components can, on the one hand, utilize their strong antioxidant capacity to scavenge the accumulated reactive oxygen species (ROS) in the intestinal mucosa induced by inflammation and the immune response and reduce the damage to intestinal epithelial cells by ROS.[9,10] On the other hand, these components can also reduce the intensity of the inflammatory response by inhibiting the production of a variety of inflammatory cytokines (*e.g.*, tumor necrosis factor-α, interleukin-1β, *etc.*).[11–13] However, despite the potential role played by active ingredients in tea in ameliorating

[a]*Tea Research Institute, Chinese Academy of Agricultural Sciences, No. 9 Meiling South Road, West Lake District, Hangzhou, Zhejiang 310008, China.*
E-mail: linzhi@tricaas.cn
[b]*College of Food Science, Southwest University, Beibei, Chongqing 400715, China.*
E-mail: zengliangbaby@126.com

† Electronic supplementary information (ESI) available: Supplementary methods: LC-MS analytical conditions, gut microbiota analysis; Table S1: Identifications of chemical components and their relative content in 2021WP and 2011WP extracts; Table S2: Identifications of intestinal metabolites in mice and their relative content in the DSS, DSS + 5-ASA, DSS + 2021WP, and DSS + 2011WP groups; Fig. S1: Venn diagram of OTU levels among the five groups; Fig. S2: The heatmap of Spearman's correlation analysis between 26 intestinal metabolites and gut microbiota. See DOI: https://doi.org/10.1039/d3fo05176e

‡ These authors contributed equally to this work.

issues such as inflammation, there is a lack of sufficient evidence to support this mechanism of action due to issues such as low bioavailability and biotoxicity.[14,15] A recently proposed hypothesis is that tea possesses prebiotic properties that exert therapeutic effects on colitis through interacting with the gut microbiota.[16,17] For example, promoting the growth of beneficial bacteria and inhibiting the reproduction of harmful bacteria can regulate the balance of the intestinal microbial community. Furthermore, modulating a certain kind of bacteria with specific functions can affect the host's metabolism.[18,19] These effects are largely dependent on the different active compounds in different teas, so supplementation with different teas affects different types of bacterial taxa in the gut.[20,21]

White tea is one of the six traditional tea categories in China. Unlike unfermented green tea and fully fermented black tea, white tea is a slightly fermented tea. Its catechin content accounts for approximately 7.26–18.48% of all components, between that of green tea (24–36%) and black tea (6%).[22] As a result of the degradation of proteins during withering, white tea is particularly rich in free amino acids, which can reach proportions of 6.0–8.9%.[23] In addition, white tea contains approximately 3–5% alkaloids, 2–9% dimeric catechins, 0.6–4.8% phenolic acids, and 0.5–1.8% flavonoid glycosides.[24] Furthermore, white tea is suitable for storage, and there has always been a tradition of storing white tea in folklore. During the storage period, ranging from several years or even decades, most of the white tea compounds such as catechins, flavonoid glycosides, and amino acids decrease gradually with storage time, but compounds such as gallic acid and *N*-ethyl-2-pyrrolidone-substituted flavan-3-ol (EPSF) increase significantly; for example, there was a decrease in catechins by approximately 18% and a 7–10-fold increase in the contents of EPSFs based on the covalent binding of catechins and theanine, and the EPSF content reached up to 0.2% after 10 years of storage.[25–27] These changes in chemical compositions can also lead to the variations in health benefits of white tea. For example, the antioxidant activity and the inhibitory effect against α-amylase and α-glucosidase decreased along with the storage of white tea.[28] Although the antioxidant, neuroprotective, antimutagenic, anticancer, and hypoglycemic effects of white tea have been demonstrated, the effect of storage on the health benefits of white tea is unknown, and in particular, the effects of white tea on the gut microbiota have rarely been reported.

In this study, we aimed to confirm the effect of stored white tea on alleviating colitis and further investigate the effects of different storage periods of white tea on the gut microbiota and its metabolites in mice. In conclusion, these results suggest that stored white tea may be a new option for the treatment of UC.

2. Materials and methods

2.1. Chemicals and reagents

Dextran sulfate sodium (DSS, MW: 36–50 kDa) was purchased from Meilun Biotechnology Co., Ltd (Dalian, China). 5-Aminosalicylic acid (5-ASA) and β-cyclodextrin were purchased from Aladdin (Shanghai, China).

Theanine and gallic acid (GA) were obtained from J&K Scientific Ltd (Beijing, China). Caffeine, epicatechin (EC), epicatechin gallate (ECG), epigallocatechin (EGC), epigallocatechin gallate (EGCG), quercetin 3-*O*-galactoside, quercetin 3-*O*-glucoside, kaempferol 3-*O*-rutinoside, myricitrin, vitexin, and isovitexin were obtained from Sigma-Aldrich (St Louis, MO, USA). Kaempferol 3-*O*-galactoside was obtained from ChemFaces (Wuhan, China). 5‴R-EGCG-8-C *N*-ethyl-2-pyrrolidinone (8-C R-EGCG-cThea) was synthesized in our laboratory.[25,27]

Taurocholic acid (TCA), α-muricholic acid (α-MCA), β-muricholic acid (β-MCA), tauro-α-muricholic acid (T-α-MCA), tauro-β-muricholic acid (T-β-MCA), and cholic acid-d4 (CA-d4) were purchased from Yuanye Bio-Technology Co., Ltd (Shanghai, China). Cholic acid (CA), lithocholic acid (LCA), and deoxycholic acid (DCA) were purchased from Apexbio (Beijing, China). Chenodeoxycholic acid (CDCA), ursodeoxycholic acid (UDCA), and tauroursodeoxycholic acid (TUDCA) were purchased from Harvey Biotechnology Co., Ltd (Beijing, China). Taurocholic acid-d4 (TCA-d4, sodium salt) was purchased from Manhage Biotechnology Co., Ltd (Beijing, China). Taurodeoxycholic acid (TDCA) was purchased from Cayman Chemical (Ann Arbor, Michigan, USA).

Acetonitrile, ammonium bicarbonate and formic acid were of liquid chromatography-mass spectrometry (LC-MS) grade and were purchased from Merck (Darmstadt, Germany), Sigma-Aldrich (St Louis, MO, USA) and TCI (Tokyo, Japan). Deionized water was produced using a Milli-Q water purification system (Millipore, Billerica, MA, USA).

2.2. Preparation of white tea extract

A 2021-produced white peony (2021 WP) and a 2011-produced white peony (2011 WP) were purchased from Fujian Pinpinxiang Tea Co., Ltd as representatives of new and 10-year stored white tea. The white tea samples were made from the fresh tea leaves (one bud and two leaves grade) of *Camellia sinensis* cv. Fuding-dabaicha plucked in April and were manufactured according to the processing procedure of GB/T 32743-2016 standard. Then, the white teas were placed in a black light-proof bag and stored in a room with a controlled environment at a temperature of 25 °C and a humidity of 50% with reference to GB/T 30375-2013. All tea samples were ground and extracted with pure water (1 : 20, w/v) at 100 °C for 30 min. After filtration, pure water (1 : 20, w/v) was added to the residue for a second extraction. The filtrate was mixed and freeze-dried and then stored at −80 °C.

2.3. Chemical composition analysis of white tea extract

An established method based on ultra high performance liquid chromatography (UHPLC)-Q-Exactive/mass spectrometry (MS) (Thermo Fisher, San Jose, CA, USA) was used to determine the chemical composition of the white tea extracts.[29] The detailed analytical conditions are provided in the ESI.†

The contents of 7 flavanols, 2 alkaloids, 8 EPSFs, 12 flavonoid glycosides, theanine and gallic acid were quantified using the external standard method. Gallocatechin gallate (GCG), gallocatechin (GC), and catechin (C) were quantified using the corresponding stereoisomers of EGCG, EGC, and EC, respectively. Theobromine was quantified by utilizing the calibration curve of caffeine. 5″R-epicatechin-8-C *N*-ethyl-2-pyrrolidinone (8-C R-EC-cThea), 5″S-epicatechin-8-C *N*-ethyl-2-pyrrolidinone (8-C S-EC-cThea), 5″R-epigallocatechin-8-C *N*-ethyl-2-pyrrolidinone (8-C R-EGC-cThea), 5″S-epigallocatechin-8-C *N*-ethyl-2-pyrrolidinone (8-C S-EGC-cThea), 5‴ R-epicatechin gallate-8-C *N*-ethyl-2-pyrrolidinone (8-C R-ECG-cThea) and 5‴ S-epicatechin gallate-8-C *N*-ethyl-2-pyrrolidinone (8-C S-EGCG-cThea) were quantified by utilizing the calibration curve of 8-C R-EGCG-cThea. Quercetin 3-*O*-rutinoside and quercetin 3-glucosylrutinoside were quantified by utilizing the calibration curve of quercetin 3-*O*-glucoside, and kaempferol 3-*O*-glucoside and kaempferol 3-glucosylrutinoside were quantified by utilizing the calibration curve of kaempferol 3-*O*-rutinoside. Myricetin 3-*O*-glucoside and myricetin 3-*O*-galactoside were quantified by utilizing the calibration curve of myricitrin. The concentration gradients of the standards were as follows: 0.05, 0.1, 0.2, 0.5 and 1 mg mL^{-1} for EGCG, ECG, EGC, EC, caffeine, theanine and 8-C R-EGCG-cThea; 0.01, 0.02, 0.05, 0.1, 0.2 and 0.5 mg mL^{-1} for gallic acid; and 0.18, 0.36, 1.8, 3.6, 18, 36, and 180 μg mL^{-1} for quercetin 3-*O*-galactoside, quercetin 3-*O*-glucoside, kaempferol 3-*O*-rutinoside, kaempferol 3-*O*-galactoside, myricitrin, vitexin, and isovitexin.

2.4. Animals and treatments

Male C57BL/6J mice (6 weeks old, 18–22 g) were purchased from Hangzhou Medical College (Hangzhou, China, Production Permit No. SCXK (Zhejiang) 2019-0002). All mice were housed in a temperature-controlled environment (23 ± 2 °C) with food and water *ad libitum* with a 12-hour light–dark cycle. All animal procedures were performed in accordance with the Guidelines for Care and Use of Laboratory Animals of Hangzhou Medical College and approved by the Animal Ethics Committee of Zhejiang Experimental Animal Center of Hangzhou Medical College (approval number: ZJCLA-IACUC-20010172). All animal experiments were performed in compliance with the relevant laws and institutional guidelines for the care and use of laboratory animals in China (GB/T 35892-2018 and GB/T 35823-2018).

After 1 week of adaptive feeding, the mice were randomly divided into the following five groups (n = 6): the CK group, the DSS group, the DSS + 5-ASA group, the DSS + 2021 WP group and the DSS + 2011 WP group. Except for the CK group, mice in all groups were fed sterile water containing 3% DSS solution for 1 week. Among them, mice in the DSS + 5-ASA group were treated with 5-ASA (100 mg kg^{-1} day^{-1}, dissolved in 2% cyclodextrin) by gavage, and mice in the DSS + 2021 WP group and DSS + 2011 WP group were treated with 2021 white peony tea extract (200 mg kg^{-1} day^{-1}) and 2011 white peony tea extract (200 mg kg^{-1} day^{-1}) by gavage, respectively. The above dose (200 mg kg^{-1} day^{-1}) is calculated according the body surface area normalization method:[30] the intake of 5 g day^{-1} of white tea in an adult human weighing 70 kg is equivalent to a dose of 880.6 mg kg^{-1} day^{-1} for mice. The normalization equation is as follows, where the Km factor is 3 for mice and 37 for human. The actual extraction rate of white tea was about 23% (the ratio of extract mass to tea mass) using the extraction method described in "2.2 Preparation of white tea extract", and the dose of white tea extract was finally calculated as 200 mg kg^{-1} day^{-1}.

$$\text{Human dose}\left(\text{mg kg}^{-1}\right) = \text{animal dose}\left(\text{mg kg}^{-1}\right) \times \frac{\text{animal Km}}{\text{human Km}}$$

After 3 days of DSS treatment, the mice were euthanized with ether. Major tissues (liver, colonic tissue and intestinal contents) were collected and stored at −80 °C for subsequent analysis.

2.5. Measurement of the disease activity index and spleen index

The body weight, anal bleeding and fecal consistency of mice were recorded daily during the animal experiments. The disease activity index (DAI) was calculated according to the following scoring system in the literature:[31] (1) no loss of body weight was scored as 0, 1 point for 1–5% weight loss, 2 points for 6–10% weight loss, 3 points for 11–20% weight loss, and 4 points for >20% weight loss; (2) no blood was scored as 0, 2 points for positive occult blood, and 4 points for gross bleeding; and (3) well-formed stool pellets were scored as 0, pasty stools but not adhering to the anus were scored as 2 points, and liquid stools were scored as 4 points.

The body weight of the mice was recorded before sacrifice, and the spleen tissue was weighed after sacrifice. The spleen index was calculated according to the ratio of spleen weight to body weight.

2.6. Histological analysis

Colon and liver tissues were cut, fixed in 4% paraformaldehyde, dehydrated with gradient concentrations of ethanol, embedded in paraffin and sectioned into 4 μm slides. The slides were stained using a hematoxylin and eosin (H&E) staining kit (Servicebio, Wuhan, China). A Nikon Eclipse E100 microscope (Nikon, Tokyo, Japan) was used to take images.

2.7. Gut microbiota analysis

The fresh fecal samples were stored at −80 °C and sent to APTBIO Biotechnology Co., Ltd (Shanghai, China) for 16S rDNA sequencing analysis. Briefly, total genomic DNA from the fecal sample was extracted using the CTAB/SDS method. DNA concentration and purity were monitored on 1% agarose gels. According to the concentration, DNA was diluted to 1 ng μL^{-1} using sterile water. 16S rDNA (V3–V4 region) was amplified using specific primers (341F: CCTACGGGNGGCWGCAG; 806R: GGACTACHVGGGTATCTAAT) *via* polymerase chain reac-

tions. The purified amplification product (amplicon) was analyzed using the NovaSeq 600 platform (Illumina, San Diego, USA). Detailed information about library construction, paired-end read assemblies, operational taxonomic unit (OTU) cluster and species annotation, α-diversity index calculation, β-diversity analysis and bacterial differential analysis is included in the ESI.†

2.8. Intestinal metabolites and content analysis of mice

Metabolite extraction was performed according to previously described methods in the literature with modification.[32] In brief, 10 mg of intestinal content sample was mixed with 1 mL of methanol/water = 2 : 1 (v/v) solution containing CA-d4 and TCA-d4 internal standards (0.2 μg mL^{-1}) and subjected to three freeze–thaw cycles in liquid nitrogen, followed by homogenization using a T18 TissueLyser (IKA, Germany) and centrifugation for 10 min at 10 000 rpm at 4 °C. Finally, the sample was passed through a 0.22 μm membrane for LC-MS analysis.

A UHPLC-Q-Exactive/MS instrument was used for analysis of the intestinal metabolites. An HSS T3 column (100 mm × 2.1 mm, 1.8 μm, Waters, Manchester, UK) was used as the chromatographic column at a temperature of 40 °C. The binary mobile phases were 10 mM ammonium bicarbonate solution (phase A) and 100% acetonitrile (phase B), and the flow rate was set at 0.2 mL min^{-1}. The gradient elution program was set as follows: 0–2 min, 5% phase B; 2–6 min, 5%–30% phase B; 6–10 min, 30%–40% phase B; 10–12 min, 40%–85% phase B; 12–12.5 min, 85%–5% phase B; and 12.5–16 min, 5% phase B. The injection volume was 3 μL. The mass spectrometer was operated in negative electrospray ionization (ESI) mode; the ionization voltage was set at 3.5 kV; the capillary temperature was 300 °C; the S-lens RF level was 50; the sheath gas flow rate was 45 L min^{-1}; the temperature and flow rate of the auxiliary gas were set at 350 °C and 10 L min^{-1}, respectively; and the MS scanning range was m/z 58–870. The contents of bile acids were quantified using the external standard method with Xcalibur 4.2 software (Thermo Fisher, San Jose, CA, USA). The calibration curves for the bile acid standards were 0.05, 0.1, 0.5, 1, 5, and 10 mg L^{-1} for LCA and DCA and 0.25, 0.5, 2.5, 5, 25, and 50 mg L^{-1} for TCA, TUDCA, T-α-MCA, T-β-MCA, TDCA, CDCA, CA, UDCA, α-MCA, β-MCA, LCA and DCA.

2.9. Statistical analysis

A supervised partial least-squares discriminant analysis (PLS-DA) and a permutation test were performed using Simca P 14.1 software (Umetrics AB, Umeå, Sweden). Independent sample t test, Kruskal–Wallis test and one-way analysis of variance (ANOVA) were performed using SPSS 17.0 (IBM, Chicago, IL, USA). Heatmap analysis was performed with MultiExperiment Viewer software (version 4.7.4, Oracle, USA) with the min-max scaling method. The data are shown as the mean ± standard deviation (SD).

3. Results and discussion

3.1. Chemical composition of 2021 WP and 2011 WP extracts

To identify the phytochemicals and other components in 2021 WP and 2011 WP, a previously established nontargeted metabolomics method was used to analyze the samples by LC-MS. After peak extraction and alignment, 3497 compound ions were obtained in positive ionization mode. Based on chemical standards, metabolomics databases (Metlin and Human Metabolome database) and our previous studies,[25,33] 82 nonvolatile compounds were identified in the 2021 WP and 2011 WP extracts, including 12 flavanols, 5 phenolic acids, 11 dimeric catechins, 14 amino acids, 2 alkaloids, 8 EPSFs, 25 flavonoid glycosides and 5 other compounds (Table S1†). Among them, 71 compounds were significantly differentially expressed ($P < 0.05$) in 2021 WP and 2011 WP, and their content distributions were depicted by a heatmap (Fig. 1).

The level of flavanols, the most abundant compounds in tea, decrease with increasing storage time.[27] Our data showed similar results; the levels of most flavanols, such as C, EC, ECG, EGCG, and GCG, were significantly lower in 2011 WP than in 2021 WP. The total amount of flavanols in 2011 WP was 360.06 mg g^{-1}, which was approximately 13.2% less than that in 2021 WP (Table 1). Not only the monomeric forms of catechins but also the dimerized catechins, such as theaflavin, theaflavin-3-gallate, and theasinensin A, were all found at lower levels in 2011 WP than in 2021 WP. It is noteworthy that the levels of the methylation product of EGCG, (−)-epigallocatechin-3-(3″-*O*-methyl) gallate (EGCG-3″-*O*-Me), increased significantly after 10 years of storage, which may be caused by microbes in the storage environment.[34]

The changes in amino acid levels during storage also tended to decrease.[27] Most of the amino acid components were found at higher levels in 2021 WP than in 2011 WP, except for aspartic acid and pyroglutamic acid. The concentration of theanine, the most abundant amino acid, was 49.06 mg g^{-1} in 2011 WP, showing a decrease of approximately 30.0% from that in 2021 WP (Table 1). However, the relative abundance of theanine-related derivatives such as EPSFs and theanine glucoside was significantly higher in 2011 WP than in 2021 WP. In particular, the EPSFs formed by the covalent combination of theanine and catechins increased to 2.07 mg g^{-1}, which was 20.1-fold higher than that in 2021 WP (Table 1).

Among the alkaloids, the contents of caffeine in 2021 WP and 2011 WP were not significantly different, while the content of theobromine was higher in 2011 WP. Theobromine is an important synthetic precursor of caffeine and a major product of caffeine degradation, and its content in 2011 WP was 2.55 mg g^{-1}, which accounted for only 1.5% of the total alkaloids (Table 1).

Kaempferol and quercetin and their primary corresponding flavonoid glycosides, such as quercetin 3-*O*-galactoside, quercetin 3-*O*-glucoside, kaempferol 3-*O*-galactoside, kaempferol 3-*O*-glucoside, quercetin 3-glucosylrutinoside, *etc*., were found at higher concentrations in 2021 WP than in 2011 WP, whereas the levels of several flavonoid glycosides, such as kaempferi-

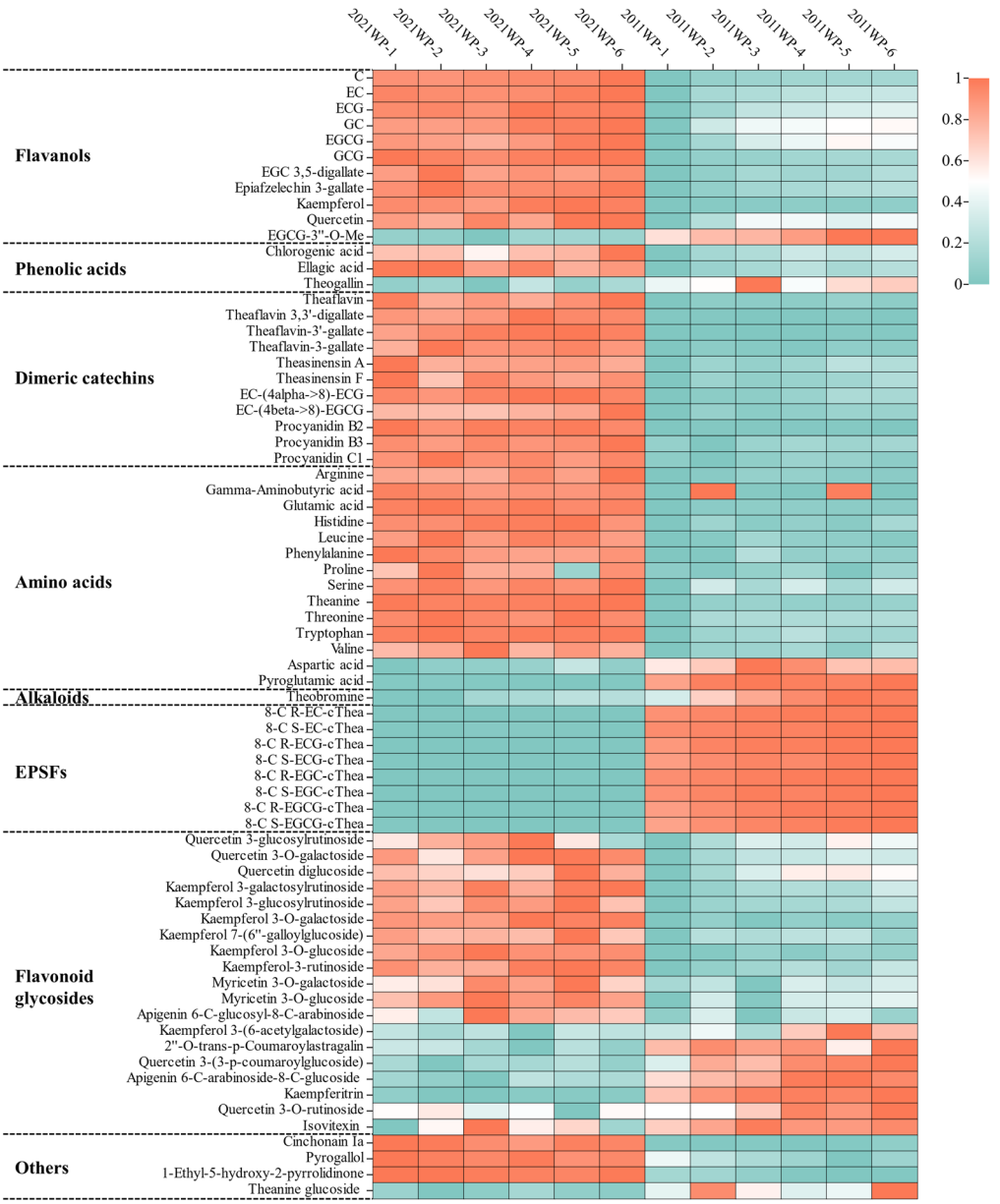

Fig. 1 Heat map of the contents of 71 significantly differential compounds in 2021WP and 2011WP extracts.

trin, quercetin 3-*O*-rutinoside, and isovitexin, exhibited the opposite trend (Table 1). The total amount of these 12 flavonoid glycosides in 2021 WP was 13.74 mg g^{-1}, which was 1.2 times higher than that in 2011 WP (Table 1).

Regarding phenolic acids, the levels of chlorogenic acid and ellagic acid were significantly lower in 2011 WP than in 2021 WP, while the theogallin content was significantly higher in 2021 WP than in 2011 WP. The level of gallic acid did not differ significantly between the two types of white teas.

3.2. The effects of 2021 WP and 2011 WP on the pathological symptoms of colitis mice

We first assessed whether 2021 WP and 2011 WP could alleviate the symptoms of colitis in DSS-treated mice. As shown in Fig. 2A, we observed that the body weight of DSS-treated mice continued to decrease rapidly after day 5, while the intake of 5-ASA, 2021WP and 2011WP were able to significantly inhibit the trend of body weight loss in mice. Compared with 5-ASA and 2021 WP, the 2011 WP treatment had a superior effect. The mean weight loss was as high as 28.7% in the DSS group, 18.6% in the DSS + 5-ASA group, 20.4% in the DSS + 2021 WP group and only 12.5% in the DSS + 2011 WP group. The disease activity index (DAI) score of the DSS-treated mice increased rapidly from day 4 (Fig. 2B), indicating that the mice began to show typical symptoms of colitis, such as diarrhea and blood in the stool; meanwhile, the DAI scores of the mice administered 5-ASA, 2021 WP and 2011 WP were lower than those of mice in the DSS group. The spleen index of mice in

Table 1 The contents of flavanols, alkaloids, EPSFs, flavonoid glycosides, theanine and gallic acid in 2021WP and 2011WP extracts

Compounds	Content/mg·g^{-1}	
	2021WP	2011WP
C**	3.51 ± 0.08	1.67 ± 0.12
EC**	20.72 ± 0.26	14.71 ± 0.80
ECG**	88.4 ± 0.80	71.82 ± 3.22
GC**	11.26 ± 0.25	8.97 ± 0.81
EGC	69.78 ± 0.91	70.10 ± 3.19
EGCG*	193.73 ± 2.22	177.34 ± 5.87
GCG**	27.39 ± 0.42	15.45 ± 0.8
Total flavanols**	414.79 ± 4.34	360.06 ± 14.61
Caffeine	163.97 ± 2.69	162.02 ± 4.10
Theobromine**	2.29 ± 0.04	2.55 ± 0.10
Total alkaloids	166.26 ± 2.71	164.57 ± 4.18
Isovitexin*	0.04 ± 0.01	0.05 ± 0
Vitexin	0.04 ± 0	0.04 ± 0
Kaempferol 3-*O*-glucoside**	0.99 ± 0.02	0.66 ± 0.02
Kaempferol 3-*O*-galactoside**	0.22 ± 0.01	0.14 ± 0
Kaempferol 3-*O*-rutinoside**	0.79 ± 0.03	0.57 ± 0.03
Kaempferol 3-glucosylrutinoside**	3.34 ± 0.11	2.62 ± 0.09
Quercetin 3-*O*-rutinoside**	0.74 ± 0.04	0.8 ± 0.04
Quercetin 3-*O*-galactoside**	3.86 ± 0.18	3.07 ± 0.15
Quercetin 3-*O*-glucoside	0.68 ± 0.13	0.62 ± 0.02
Quercetin 3-glucosylrutinoside*	1.99 ± 0.12	1.84 ± 0.08
Myricetin 3-*O*-glucoside**	0.59 ± 0.01	0.52 ± 0.02
Myricetin 3-*O*-galactoside**	0.46 ± 0.03	0.36 ± 0.02
Total flavonoid glycosides**	13.74 ± 0.38	11.28 ± 0.43
8-C R-EC-cThea**	0.02 ± 0	0.25 ± 0.01
8-C R-ECG-cThea**	0.01 ± 0	0.15 ± 0.01
8-C R-EGC-cThea**	0.01 ± 0	0.20 ± 0.01
8-C R-EGCG-cThea**	0.03 ± 0	0.74 ± 0.04
8-C S-EC-cThea**	0.02 ± 0	0.20 ± 0.01
8-C S-ECG-cThea**	0.004 ± 0	0.11 ± 0.01
8-C S-EGC-cThea**	0.01 ± 0	0.17 ± 0.01
8-C S-EGCG-cThea**	0.01 ± 0	0.26 ± 0.01
Total EPSFs**	0.10 ± 0	2.07 ± 0.09
Gallic acid	52.86 ± 2.39	57.47 ± 9.23
Theanine**	70.12 ± 0.35	49.06 ± 0.84

*$P < 0.05$, **$P < 0.01$, determined by independent sample *t*-test.

the DSS group was significantly higher than that in the CK group due to hemorrhage and swelling of the spleen caused by DSS treatment, while the spleen index of mice treated with 5-ASA, 2021 WP and 2011 WP was significantly lower than that of mice in the DSS group (Fig. 2C). In addition, the length and appearance of the mouse colon revealed that DSS treatment induced significant shortening and hemorrhage of the colon, in contrast to what was seen in the CK group. Both the 2021 WP and 2011 WP treatments significantly limited the shortening of colon length, and 2011 WP was slightly more effective than 2021 WP (Fig. 2D and E). H&E staining results indicated that the intestine of DSS-treated mice was significantly impaired compared with that of mice in the CK group, as evidenced by a reduced number of goblet cells, reduced inflammatory cell infiltration, and lower levels of structural damage to the colonic crypt and intestinal villi (Fig. 2F). However, administration of 5-ASA, 2021 WP, and 2011 WP significantly improved the pathologic features of the colon and protected the structure of the colonic crypts and villi (Fig. 2F). In addition, liver pathology caused by DSS (*e.g.*, hepatocyte destruction, liver inflammation and enlargement) was also reduced by treatment with stored white tea (Fig. 2G). These results demonstrated that the administration of 2021 WP and 2011 WP alleviated the pathological symptoms of DSS-induced colitis in mice, with 2011 WP treatment leading to slightly better improvement than 2021 WP treatment. The aforementioned chemical analysis results showed that the compound contents of EPSFs, theobromine, and EGCG-3″-*O*-Me were significantly higher in 2011WP than in 2021WP. Especially, EPSFs were reported to have higher anti-inflammatory effect than EGCG and theanine by modulating NF-κB signalling pathway;[26] EGCG-3″-*O*-Me was reported to have a 2.5 times higher bioavailability than that of EGCG[35] and possesses multiple benefits such as anti-fatigue, cardiovascular disease risk prevention, anti-obesity, and gut microbiota regulation.[36] These compounds may play an important role in alleviating colitis pathology due to their exceptional biological activities.

3.3. The effects of 2021 WP and 2011 WP on the gut microbiota of colitis mice

To investigate whether 2021 WP and 2011 WP alleviated colitis by modulating the gut microbiota, we characterized the structure of the gut microbiota of 25 samples from the 5 experimental groups based on the V3–V4 variable region by 16S rDNA gene sequencing. A total of 770, 709, 735, 773 and 681 OTUs were identified in the stool samples from the CK, DSS, DSS + 5-ASA, DSS + 2021 WP and DSS + 2011 WP groups, respectively (Fig. S1†). Among them, 401 OTUs were common in the 5 groups (Fig. S1†). Then, the species diversity in the microbiome was assessed based on the observed species index, the PD_whole_tree index, the Chao1 index and the Ace index, and there was no significant difference among the 5 groups (Fig. 3A–D). Furthermore, PCoA analysis was performed at the OTU level to assess the overall microbial structure. As shown in Fig. 3E, there was significant separation among the CK, DSS, and DSS + 2011 WP groups, but some degree of overlap among the DSS, DSS + 5-ASA, and DSS + 2021 WP groups. Next, we analyzed the species and relative abundance (top 10) of the gut microbiota in the 5 groups. At the phylum level, DSS treatment caused a significant increase in the relative abundance of *p_Proteobacteria* and a significant decrease in the relative abundance of *p_Patescibacteria* and *p_Actinobacteria* in the feces of mice (Fig. 3F). The administration of 5-ASA, 2021 WP and 2011 WP significantly reversed the increase in the abundance of *p_Proteobacteria* caused by DSS but had no effect on the decrease in the abundance of *p_Actinobacteria* and *p_Patescibacteria* (Fig. 3H–J). At the genus level, the relative abundance of *g_Bacteroides*, *g_Parabacteroides* and *g_Escherichia-Shigella* in the feces of mice in the DSS group was significantly higher than that in the CK group, and the relative abundance of *g_Candidatus Saccharimonas* was significantly lower than that in the CK group (Fig. 3G). In particular, enrichment of the harmful bacteria *g_Bacteroides* and *g_Escherichia-Shigella* was strongly associated with the aggravation of ulcerative colitis. For instance, an excessive amount of the proteases secreted by *g_Bacteroides* are related to worsening ulcerative colitis.[37]

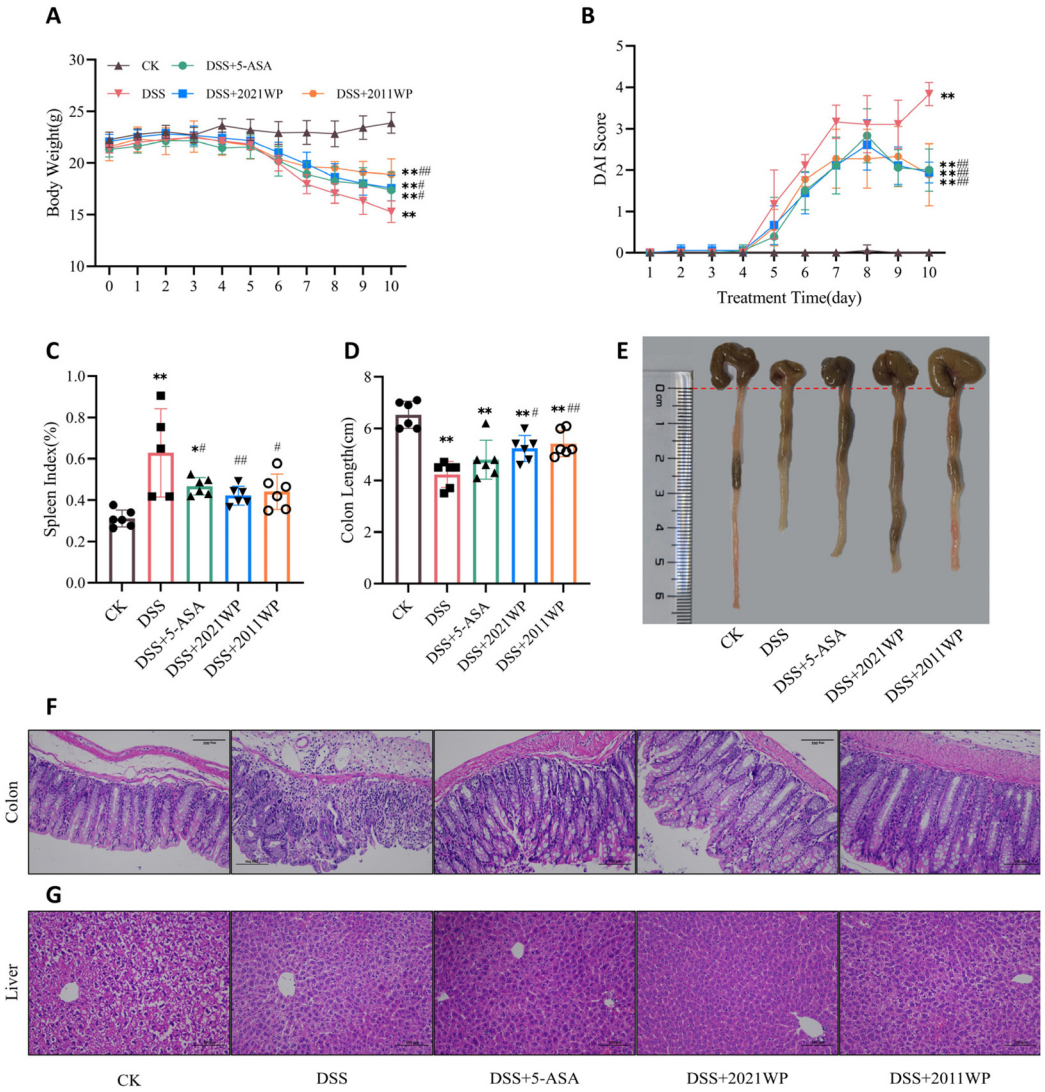

Fig. 2 2021 WP and 2011 WP alleviation of the pathological symptoms of DSS-induced colitis in mice. (A) Body weight changes; (B) the disease activity index (DAI) score; (C) the spleen index; and (D) the colon length were determined. (E) The colon samples were also photographed. Morphological analysis of hematoxylin–eosin (H&E) staining of colon (F) and liver (G) tissues was performed (scale bar = 200 μm, magnification of the microphotograph, 100×). Data are presented as the mean ± SD (n = 6). *P < 0.05, **P < 0.01, *vs.* CK group; and #P < 0.05, ##P < 0.01, *vs.* DSS group, as determined by one-way ANOVA with Dunnett's multiple comparison test.

Linear discriminant analysis (LDA) also showed that *g_Bacteroides* and *g_Escherichia-Shigella* were the differentially abundant bacterial taxa of the DSS group (Fig. 4). The abundance of *g_Bacteroides* in the feces of mice treated with 5-ASA, 2021 WP, and 2011 WP was significantly reduced by 37.6%, 45.9%, and 71.4%, respectively, compared with that in the DSS group (Fig. 3K). In addition, the abundance of *g_Escherichia-Shigella* in the feces of mice treated with 5-ASA and 2011 WP was significantly reduced by 76.2% and 92.0%, respectively, compared with that in the DSS group (Fig. 3M). These results are consistent with reports that the administration of fuzhuan brick tea significantly inhibited the relative abundance of both *g_Bacteroides* and *g_Escherichia-Shigella*, and the intake of Tieguanyin oolong tea reduced the abundance of *g_Escherichia-Shigella* by about 20%.[38,39] There were no significant differences in the abundance of *g_Parabacteroides* (Fig. 3L) or *g_Candidatus Saccharimonas* in the 5-ASA-, 2021 WP-, and 2011 WP-treated groups compared with that in the DSS group (Fig. 3N).

LEfSe analysis was performed on the samples according to different grouping conditions based on taxonomic composition to identify the communities or species that had a significant effect on the division of the samples. The communities or species with LDA values greater than 3 were identified as the bacterial taxa with the most substantial abundance differences (Fig. 4). *f_Muribaculacea*, *g_Achromobactel*, *g_Enterorhabdus*, *f_Eggerthellacea*, *c_Coriobacteriia*, *o_Coriobacteriales*, *g_Pseudomonas*, and *f_Pseudomonadaceae* were identified as differentially abundant bacterial taxa in the CK group. Differentially abundant bacterial taxa in the DSS group were *g_Bacteroides* and *g_Escherichia Shigella*, *f_Bacteroidaceae*, *c_Alphaproteobacteria*,

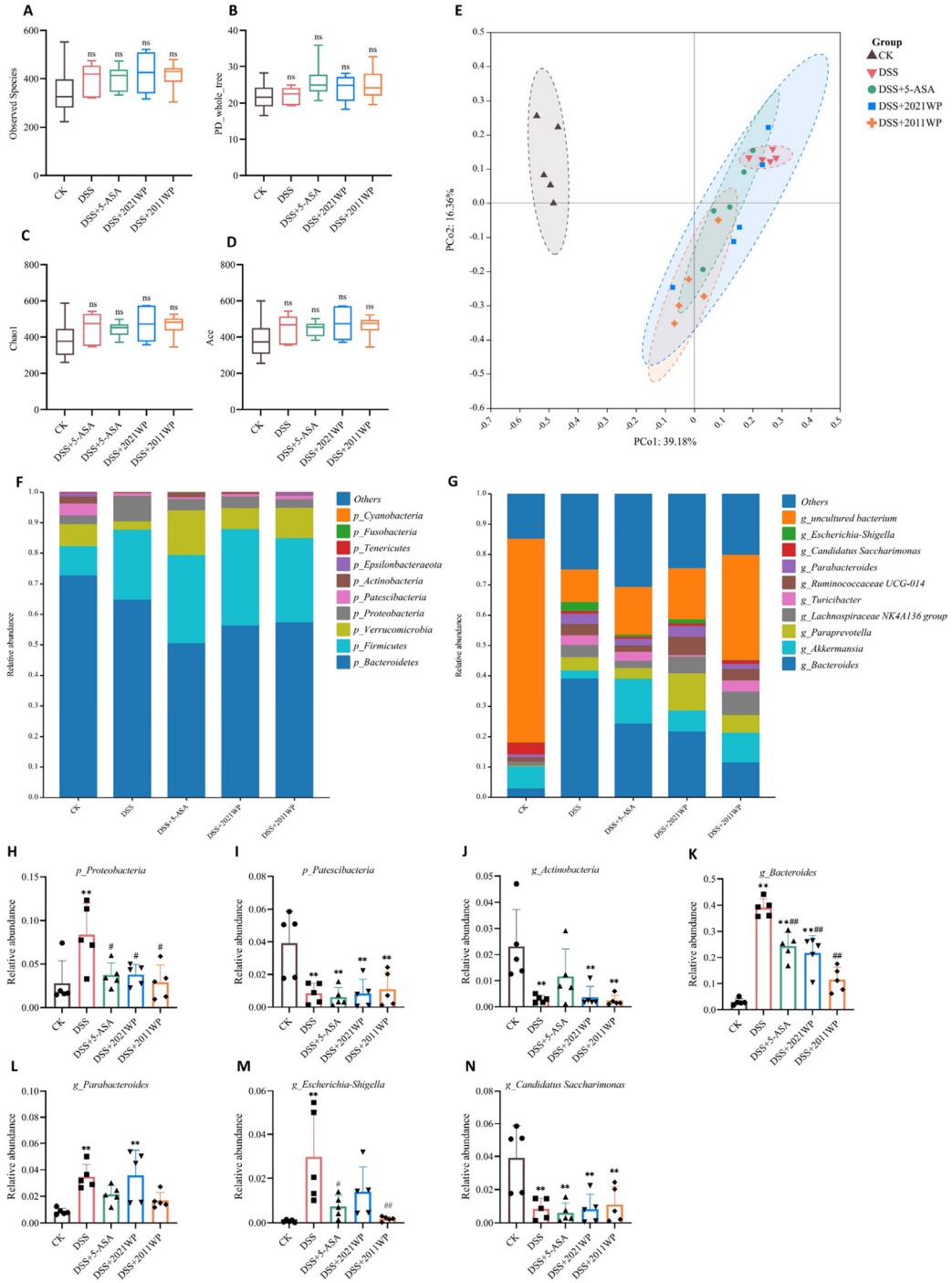

Fig. 3 Effect of the intake of 2021 WP and 2011 WP on the gut microbiota of DSS-induced mice. (A–D) α-Diversity was represented by violin plots of the Observed_species index, the PD_whole_tree index, the Chao1 index and the Ace index. (E) PCoA plot of gut microbiota was based on weighted UniFrac distance. (F and G) Plots of the top 10 structural components of the gut microbiota community in terms of relative abundance at the phylum level (F) and genus level (G) are shown. (H–N) Changes in the relative abundance of microbial communities with significantly different abundances in the DSS group after 5-ASA, 2021 WP, and 2011 WP treatments at the phylum level (H–J) and genus level (K–N) are shown. Data are presented as the mean ± SD (n = 5). ns, not significant; *P < 0.05, **P < 0.01, *vs.* CK group; and #P < 0.05, ##P < 0.01, *vs.* DSS group, as determined by one-way ANOVA with Tukey's multiple comparison test.

o_Rhodospirillales, *o_Enterobacteriales* and *f_Enterobacteriaceae*. Among them, *c_Alphaproteobacteria*, *o_Rhodospirillales*, *o_Enterobacteriales* and *f_Enterobacteriaceae* all belong to *p_Proteobacteria*, while *p_Proteobacteria* was the most abundant in the DSS group among the five groups (Fig. 3H). *g_Flavonifractor*, *g_Faecalitalea*, *f_Burkholderiaceae*, and *o_Betaproteobacteriales*

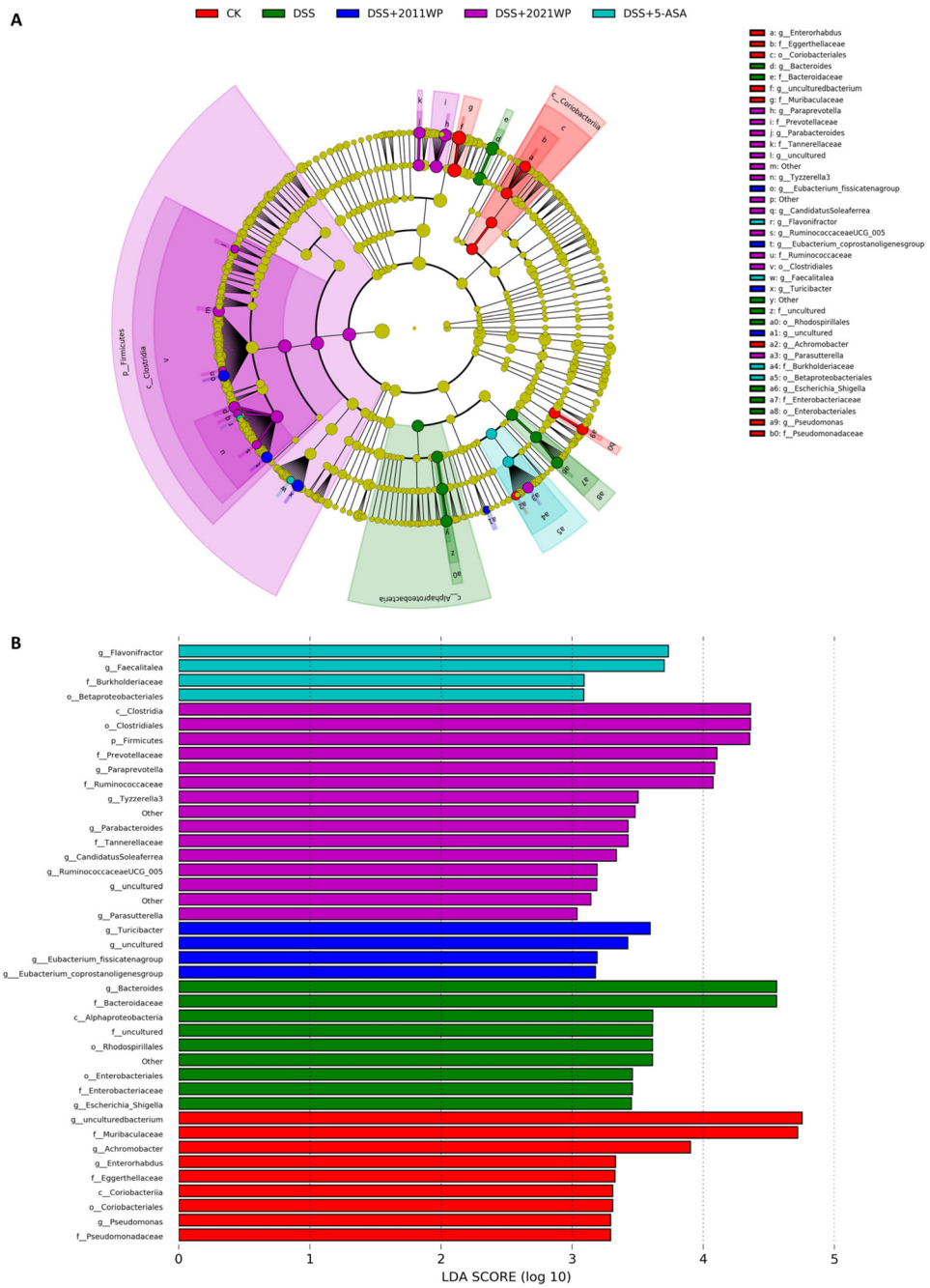

Fig. 4 Identification of the characteristic gut bacterial taxa among the five groups. (A) Analysis of the differentially abundant bacterial taxa among the five groups by LEfSe. The circles radiating from inside to outside in the cladogram represent the taxonomic levels from phylum to genus, and the nodes with different colors represent the microbial communities with significant roles in the grouping. (B) Differentially abundant bacterial taxa based on LDA with a threshold score > 3.0 (n = 5).

were identified as differentially abundant bacterial taxa in the DSS + 5-ASA group. The highest number of differentially abundant bacterial taxa was identified in the DSS + 2021 WP group, and these taxa included *c_Clostridia*, *o_Clostridiales*, *p_Firmicutes*, *f_Prevotellaceae*, *g_Paraprevotella*, *f_Ruminococcaceae*, *g_Tyzzerella3*, *g_Parabacteroides*, *f_Tannerellaceae*, *g_Candidatus Soleaferrea*, *g_RuminococcaceaeUCG_005*, and *g_Parasutterella*. In particular, *g_Parabacteroides* had the highest abundance in the feces of mice in the DSS + 2021 WP group, which was even higher than that in the DSS group (Fig. 3L). Compared with 2021 WP treatment, 2011 WP treatment had a more substantial beneficial effect in restoring gut microbial dysbiosis induced by DSS. The differentially abundant bacterial taxa in the DSS + 2011 WP group were mainly *g_Turicibacter*, *g_Eubacterium_fissicatenagroup* and *g_Eubacterium_coprostanoligenesgroup*. Notably, *g_Turicibacter* influences a wide range of host metabolites, including lipids and

bile acids.[40] Therefore, we next analyzed the microbial metabolites in the colonic contents of mice with colitis.

3.4. The effects of 2021 WP and 2011 WP on intestinal metabolites in colitis mice

The colon contents of mice were analyzed by LC-MS. Twenty-six intestinal metabolites, including 5 short-chain fatty acids, 12 bile acids, 8 amino acids, and 1 other compound, were identified based on chemical standards and metabolomic databases (Metlin and the Human Metabolome database) (Table S2†). PLS-DA showed that the CK group showed a clear trend of separation from the other groups in the direction of principal component 1, while the DSS + 5-ASA, DSS + 2021 WP, and DSS + 2011 WP groups all showed separation from the DSS group (Fig. 5A), indicating that the 5-ASA, 2021 WP, and 2011 WP treatments all partially alleviated the intestinal metabolite disorder induced by DSS, although the metabolism levels in these 3 groups still differed from those of healthy mice. The 200-permutation test showed that the intercepts of R2 and Q2 were 0.0775 and −0.211, respectively, which indicated that the PLS-DA model was reliable (Fig. 5B). The variable importance in projection (VIP) was calculated, and the metabolites with VIP greater than 1 and P value less than 0.05 were identified as the key differentially abundant compounds (Table S2†). The levels of the 10 key differentially abundant compounds in the samples are presented in Fig. 5C.

Short-chain fatty acids are saturated carboxylic acids with one to six carbon chains that are produced by the fermentation of dietary fibers in food by the gut microbiota; these fatty acids are an important energy source for colonic epithelial cells and possess physiological functions such as promoting intestinal mucosal barrier integrity, inhibiting the inflammatory response and increasing nutrient absorption.[41,42] Fig. 5C shows that butyric acid, isobutyric acid and isovaleric acid, which are among the short-chain fatty acids, were identified as key differentially abundant metabolites; their levels were significantly higher in the intestinal contents of mice in the DSS + 5-ASA, DSS + 2021 WP, and DSS + 2011 WP groups compared with that in the DSS group, although they were still significantly lower than the levels in the CK group. Amino acids in the colon are produced from dietary protein degradation by intestinal microorganisms and are also small molecules with various physiological functions, such as promoting intestinal growth and maintaining mucosal integrity and barrier function.[43,44] Individual amino acids, such as glutamic acid, arginine and tryptophan, also play significant roles in reducing inflammation, oxidative stress and the level of proinflammatory cytokines.[45–47] Fig. 5C shows that threonine was most abundant in the CK group and was slightly more abundant in the DSS + 5-ASA, DSS + 2021 WP and DSS + 2011 WP groups compared with that in the DSS group.

Bile acids are a class of compounds with a steroidal structure that are synthesized by liver cells and released into the intestines *via* the gallbladder.[48] The primary role of bile acids

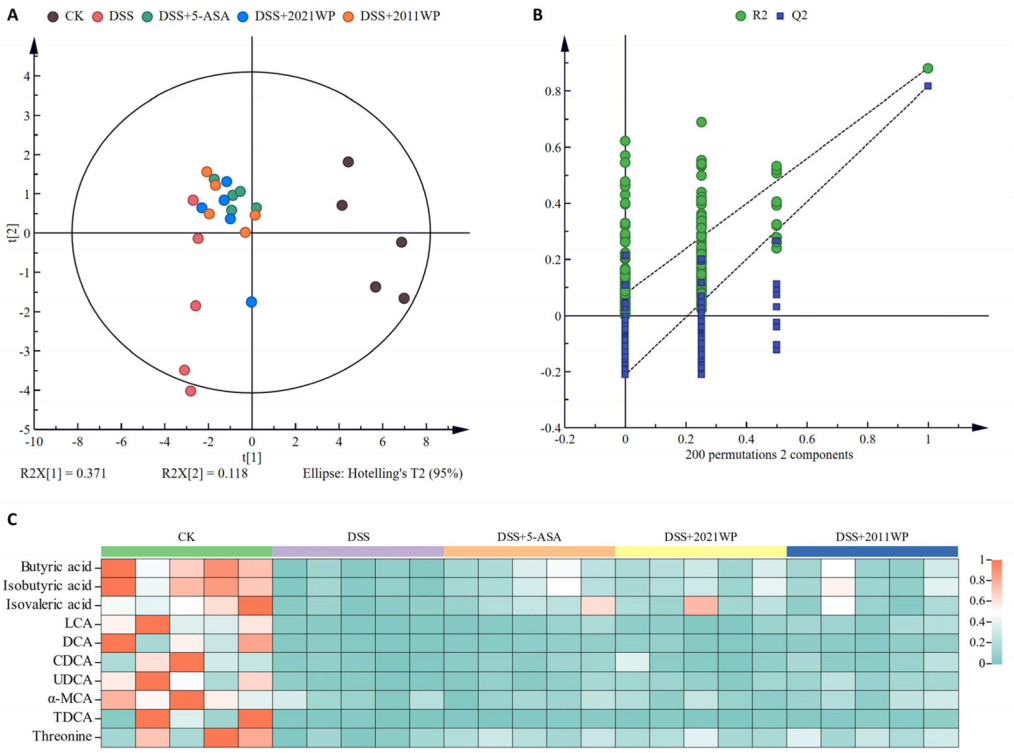

Fig. 5 Effect of the intake of 2021 WP and 2011 WP on intestinal metabolites in DSS-induced mice. (A) PLS-DA of intestinal metabolites in the colon contents of mice among the five groups was performed. (B) Cross-validation plot of the PLS-DA model with 200 permutation tests is shown. (C) The heatmap shows changes in the content of key differentially abundant compounds (VIP > 1 and P < 0.05) among the 5 groups.

is to assist in fat digestion and absorption in the small intestine. Recent studies have shown that approximately 5% of bile acids, after exocytosis into the colon, transform into secondary bile acids and undergo sulfation, dehydroxylation, and isomerization by gut microbes; these secondary bile acids act as signaling molecules in bile acid metabolism regulation, lipid and glucose homeostasis, inflammatory response modulation, barrier function, and the prevention of intestinal bacterial translocation.[49–51] Fig. 5 and Table 2 show that the primary bile acids CDCA, UDCA, and α-MCA and the secondary bile acids LCA, DCA, and TDCA were differentially abundant metabolites when comparing the different groups. These bile acid metabolites all showed the highest levels in the CK group, and there were no significant differences in the levels of these metabolites between the DSS, DSS + 5-ASA, DSS + 2021 WP and DSS + 2011 WP groups. The quantitative results in Table 2 show that the level of primary bile acids was higher than that of secondary bile acids in the colonic contents of mice in different experimental groups, and the ratio of primary bile acids to secondary bile acids was significantly lower in the CK, DSS + 5-ASA, and DSS + 2011 WP groups than in the DSS group. These results suggested that gut microbial disorder caused by DSS attenuated the conversion of bile acids from primary to secondary types, and the intake of both 2011 WP and 5-ASA significantly reversed this trend.

3.5. Correlation of the gut microbiota and intestinal metabolites

The relationships between intestinal metabolites and gut microbial taxa (genus level) were explored by Spearman's correlation analysis (Fig. S2† and Fig. 6). The results showed that short-chain fatty acids were generally negatively correlated with 17 microbes. In particular, 6 microbes, *g_Bacteroides*, *g_Romboutsia*, *g_Parabacteroides*, *g_Ruminococcaceae UCG-014*, *g_Turicibacter*, and *g_Alistipes*, had significant negative correlation coefficients with all short-chain fatty acids (Fig. S2† and Fig. 6). The microbes with positive correlations with short-chain fatty acids were *g_Candidatus Saccharimonas*, *g_Akkermansia*, *g_Pseudomonas*, *g_Enterorhabdus*, *g_Dubosiella*, and *g_Lactobacillus* (Fig. S2†). Among them, *g_Candidatus Saccharimonas* and *g_Enterorhabdus* were significantly positively correlated with both of the important differentially abundant metabolites butyric acid and isobutyric acid (Fig. 6), which play crucial roles in maintaining intestinal barrier func-

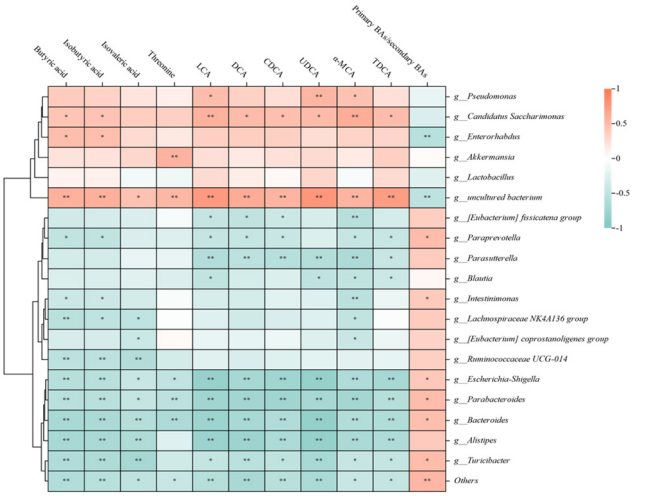

Fig. 6 Heatmap of Spearman's correlation analysis of intestinal metabolites and gut microbiota. Different colors represent the value of the correlation coefficient; red indicates a positive correlation, and blue indicates a negative correlation. *P < 0.05, **P < 0.01.

Table 2 The contents of bile acids in the CK, DSS, DSS + 5-ASA, DSS + 2021WP, and DSS + 2011WP groups

	Content/nmol·g^{-1}				
Metabolites	CK	DSS	DSS + 5-ASA	DSS + 2021WP	DSS + 2011WP
Primary BAs					
CA	39.83 ± 13.37a	30.17 ± 3.69a	37.41 ± 12.91a	31.92 ± 3.99a	29.26 ± 2.02a
CDCA	8.87 ± 6.22a	0.56 ± 0.53b	1.56 ± 0.68b	2.02 ± 2.95b	2.16 ± 1.47b
UDCA	96.9 ± 51.57a	5.67 ± 3.89b	12.93 ± 8.14b	17.42 ± 6.83b	24.66 ± 8.83b
CA	39.83 ± 13.37a	30.17 ± 3.69a	37.41 ± 12.91a	31.92 ± 3.99a	29.26 ± 2.02a
α-MCA	1173.33 ± 401.7a	342.89 ± 221.6b	273.26 ± 156.03b	281.45 ± 150.5b	362.58 ± 174.25b
β-MCA	330.59 ± 166.38a	531.37 ± 489.15a	207.43 ± 108.7a	276.56 ± 113.21a	289.42 ± 146.83a
TCDCA	2.5 ± 1.76a	0.57 ± 0.17b	0.88 ± 0.3b	1.18 ± 1.04ab	1.35 ± 0.77ab
TCA	29.58 ± 12.06a	16.97 ± 1.43b	25.07 ± 9.46ab	21.81 ± 4.56ab	19.76 ± 2.36ab
T-β-MCA	70.91 ± 22.99a	94.58 ± 47.94a	67.39 ± 7.25a	103.88 ± 47.53a	74.23 ± 11.28a
T-α-MCA	73.94 ± 18.39a	58.97 ± 7.53a	52.32 ± 2.58a	76.09 ± 38.12a	58.84 ± 7.15a
Total primary BAs	1826.45 ± 372.04a	1081.73 ± 616.37b	678.25 ± 256.3b	812.33 ± 266.49b	862.26 ± 323.38b
Secondary BAs					
LCA	83.32 ± 31.46a	21.48 ± 2.7b	27.06 ± 6.5b	24.14 ± 4.55b	33.14 ± 7.15b
DCA	418.41 ± 265.68a	10.62 ± 11.38b	34.18 ± 16.53b	30.88 ± 22.02b	34.08 ± 12.93b
TDCA	31.25 ± 5.46a	26.9 ± 0.87b	26.86 ± 1.13b	26.14 ± 1.33b	25.74 ± 1.01b
Total secondary BAs	532.98 ± 257.01a	59 ± 14.34b	88.1 ± 22.24b	81.16 ± 24.84b	92.96 ± 20.35b
Ratio of primary to secondary BAs	4.15 ± 1.99b	18.6 ± 10.69a	7.59 ± 1.37b	11.26 ± 6.51ab	9.05 ± 1.94b

Significant difference (P < 0.05) was observed between the samples labeled with different small letters (one-way ANOVA with Duncan multiple comparison test).

tion, inhibiting the release of inflammatory cytokines, and promoting the homeostasis of immune cells.[52] The important differentially abundant amino acid metabolite threonine was positively correlated with *g_Akkermansia* and negatively correlated with *g_Bacteroides*, *g_Escherichia-Shigella*, *g_Parabacteroides*, and *g_Turicibacter*. Except for T-α-MCA, T-β-MCA, and β-MCA, most bile acids were positively correlated with 17 microbial species, including *g_Bacteroides*, *g_Escherichia-Shigella*, *g_Parabacteroides*, *g_Ruminococcaceae UCG-014*, and *g_Alistipes*, and positively correlated with 9 microbial species, including *g_Candidatus Saccharimonas*, *g_Akkermansia*, and *g_Lactobacillus* (Fig. S2†). Among the differentially abundant metabolites, the important bile acids were all significantly positively correlated with *g_Candidatus Saccharimonas* and significantly negatively correlated with *g_Bacteroides*, *g_Escherichia-Shigella*, *g_Parabacteroides*, *g_Turicibacter*, and *g_Alistipes* (Fig. 6). In contrast, the ratio of primary to secondary bile acids was significantly positively correlated with *g_Bacteroides*, *g_Escherichia-Shigella*, *g_Parabacteroides*, and *g_Turicibacter* but significantly negatively correlated with *g_Enterorhabdus* (Fig. 6). Secondary bile acids, especially the highly abundant LCA and DCA, are the most potent stimulators of a variety of receptors, including nuclear farnesoid X receptor (FXR), Takeda G-coupled receptor 5 (TGR5), and vitamin D receptor (VDR), which are widely expressed in colonic epithelial cells, immune cells, and colonic innervation neurons and control the host's bile acid metabolism levels, inflammatory response, and intestinal motility.[53–55] For example, in studies on mice, LCA was found to modulate colonic FOXP3$^+$ T_{reg} cells expressing RORγ through VDR and ameliorate host susceptibility to colitis.[56]

4. Conclusions

In this study, there were significant decreases in the levels of flavanols, dimeric catechins, phenolic acids, amino acids, and flavonoid glycosides in the extract of 2011 WP stored for 10 years, and significantly higher levels of EPSFs, theobromine, EGCG-3″-*O*-Me, and theogallin in the extract of 2021 WP stored for 0 years. Among these compounds, the total amount of EPSFs increased 20.7-fold in 2011 WP compared with that in 2021 WP. Intake of 200 mg kg^{-1} day^{-1} 2021 WP or 2011 WP extract significantly inhibited DSS-induced pathological features such as body weight loss, disease activity index, swelling of the spleen, colonic length atrophy, hemorrhage, and swelling and attenuation of the damage to colonic and liver tissues in mice. 2011 WP more effectively ameliorated colitis than 2021 WP, based on reversing DSS-induced gut microbiota disorder (*e.g.*, significantly suppressing the increase in the relative abundance of *g_Bacteroides* and *g_Escherichia-Shigella*) and intestinal metabolite dysregulation (*e.g.*, facilitating the conversion of primary bile acids to secondary bile acids). This study demonstrated that white tea has an effect on alleviating colitis and that storage can enhance the bioactivity of white tea.

Author contributions

Conceptualization, Zhiyuan Lin, Zhi Lin and Liang Zeng; methodology, Zhiyuan Lin, Weidong Dai and Dan Chen; validation, Zhiyuan Lin and Shanshan Hu; resources, Weidong Dai; data curation, Zhiyuan Lin; writing – original draft preparation, Zhiyuan Lin; writing – review and editing, Zhiyuan Lin and Weidong Dai; visualization, Zhiyuan Lin and Han Yan; supervision, Liang Zeng and Zhi Lin; funding acquisition, Zhi Lin and Weidong Dai. All authors have read and agreed to the published version of the manuscript.

Conflicts of interest

There are no conflicts to declare.

Acknowledgements

This research was funded by the National Natural Science Foundation of China (32272774), the Zhejiang Province Natural Science Foundation (LR23C160002), the Science and Technology Innovation Project of Chinese Academy of Agricultural Sciences (CAAS-ASTIP-2023-TRICAAS). We appreciate the analytical technique support from Instrumental Analysis Center of Tea Research Institute Chinese Academy of Agricultural Sciences.

References

1 R. B. Sartor, Mechanisms of disease: pathogenesis of Crohn's disease and ulcerative colitis, *Nat. Clin. Pract. Gastroenterol. Hepatol.*, 2006, **3**, 390–407.
2 R. J. Xavier and D. K. Podolsky, Unravelling the pathogenesis of inflammatory bowel disease, *Nature*, 2007, **448**, 427–434.
3 D. V. Bunt, A. J. Minnaard and S. El Aidy, Potential modulatory microbiome therapies for prevention or treatment of inflammatory bowel diseases, *Pharmaceuticals*, 2021, **14**, 508.
4 S. S. Seyedian, F. Nokhostin and M. D. Malamir, A review of the diagnosis, prevention, and treatment methods of inflammatory bowel disease, *J. Med. Life*, 2019, **12**, 113–122.
5 F. A. Moura, K. Q. de Andrade, J. C. F. dos Santos, O. R. P. Araújo and M. O. F. Goulart, Antioxidant therapy for treatment of inflammatory bowel disease: Does it work?, *Redox Biol.*, 2015, **6**, 617–639.
6 M. Fakhoury, R. Negrulj, A. Mooranian and H. Al-Salami, Inflammatory bowel disease: clinical aspects and treatments, *J. Inflamm. Res.*, 2014, **7**, 113–120.
7 Y. Liu, X. Wang, Q. Chen, L. Luo, M. Ma, B. Xiao and L. Zeng, *Camellia sinensis* and *Litsea coreana* ameliorate intestinal inflammation and modulate gut microbiota in

dextran sulfate sodium-induced colitis mice, *Mol. Nutr. Food Res.*, 2020, **64**, 1900943.

8 Z. Zeng, Z. Xie, G. Chen, Y. Sun, X. Zeng and Z. Liu, Anti-inflammatory and gut microbiota modulatory effects of polysaccharides from Fuzhuan brick tea on colitis in mice induced by dextran sulfate sodium, *Food Funct.*, 2022, **13**, 649–663.

9 A. G. Geagea, M. Rizzo, A. Eid, I. H. Hussein, Z. Zgheib, M. N. Zeenny, R. Jurjus, M. L. Uzzo, G. F. Spatola, G. Bonaventura, A. Leone, L. Massaad-Massade and A. Jurjus, Tea catechins induce crosstalk between signaling pathways and stabilize mast cells in ulcerative colitis, *J. Biol. Regul. Homeostatic Agents*, 2017, **31**, 865–877.

10 S. U. Rahman, Y. Li, Y. Y. Huang, L. Zhu, S. B. Feng, J. J. Wu and X. C. Wang, Treatment of inflammatory bowel disease via green tea polyphenols: possible application and protective approaches, *Inflammopharmacology*, 2018, **26**, 319–330.

11 M. Shi, Z. S. Wang, L. Y. Huang, J. J. Dong, X. Q. Zheng, J. L. Lu, Y. R. Liang and J. H. Ye, Utilization of albumin fraction from defatted rice bran to stabilize and deliver (--)-epigallocatechin gallate, *Food Chem.*, 2020, **311**, 125894.

12 M. Zeinali, S. A. Rezaee and H. Hosseinzadeh, An overview on immunoregulatory and anti-inflammatory properties of chrysin and flavonoids substances, *Biomed. Pharmacother.*, 2017, **92**, 998–1009.

13 L. Chen, Q. You, L. Hu, J. Gao, Q. Q. Meng, W. T. Liu, X. F. Wu and Q. Xu, The antioxidant procyanidin reduces reactive oxygen species signaling in macrophages and ameliorates experimental colitis in mice, *Front. Immunol.*, 2018, **8**, 1910.

14 T. Zhao, C. Li, S. Wang and X. Song, Green Tea (*Camellia sinensis*): A Review of its phytochemistry, pharmacology, and toxicology, *Molecules*, 2022, **27**, 3909.

15 Z. Cai, X. Li, J. Liang, L. Xiang, K. Wang, Y. Shi, R. Yang, M. Shi, J. Ye, J. Lu, X. Zheng and Y. Liang, Bioavailability of tea catechins and its improvement, *Molecules*, 2018, **23**, 2346.

16 Y. Liu, L. Luo, Y. Luo, J. Zhang, X. Wang, K. Sun and L. Zeng, Prebiotic properties of green and dark tea contribute to protective effects in chemical-induced colitis in mice: A fecal microbiota transplantation study, *J. Agric. Food Chem.*, 2020, **68**, 6368–6380.

17 W. W. Zhang, S. Z. Qi, X. F. Xue, Y. Al Naggar, L. M. Wu and K. Wang, Understanding the gastrointestinal protective effects of polyphenols using foodomics-based approaches, *Front. Immunol.*, 2021, **12**, 671150.

18 F. Huang, X. Zheng, X. Ma, R. Jiang, W. Zhou, S. Zhou, Y. Zhang, S. Lei, S. Wang, J. Kuang, X. Han, M. Wei, Y. You, M. Li, Y. Li, D. Liang, J. Liu, T. Chen, C. Yan, R. Wei, C. Rajani, C. Shen, G. Xie, Z. Bian, H. Li, A. Zhao and W. Jia, Theabrownin from Pu-erh tea attenuates hypercholesterolemia via modulation of gut microbiota and bile acid metabolism, *Nat. Commun.*, 2019, **10**, 4971.

19 Z. H. Ran, C. Chen and S. D. Xiao, Epigallocatechin-3-gallate ameliorates rats colitis induced by acetic acid, *Biomed. Pharmacother.*, 2008, **62**, 189–196.

20 Z. Liu, M. E. Bruins, L. Ni and J.-P. Vincken, Green and black tea phenolics: Bioavailability, transformation by colonic microbiota, and modulation of colonic microbiota, *J. Agric. Food Chem.*, 2018, **66**, 8469–8477.

21 M. A. S. Khairudin, A. M. M. Jalil and N. Hussin, Effects of polyphenols in tea (*Camellia sinensis* sp.) on the modulation of gut microbiota in human trials and animal studies, *Gastroenterol. Insights*, 2021, **12**, 202–216.

22 L. S. Lee, Y. C. Kim, J. D. Park, Y. B. Kim and S. H. Kim, Changes in major polyphenolic compounds of tea (*Camellia sinensis*) leaves during the production of black tea, *Food Sci Biotechnol*, 2016, **25**, 1523–1527.

23 Q. Chen, J. Shi, B. Mu, Z. Chen, W. Dai and Z. Lin, Metabolomics combined with proteomics provides a novel interpretation of the changes in nonvolatile compounds during white tea processing, *Food Chem.*, 2020, **332**, 127412.

24 J. Tan, U. H. Engelhardt, Z. Lin, N. Kaiser and B. Maiwald, Flavonoids, phenolic acids, alkaloids and theanine in different types of authentic Chinese white tea samples, *J. Food Compos. Anal.*, 2017, **57**, 8–15.

25 W. Dai, J. Tan, M. Lu, Y. Zhu, P. Li, Q. Peng, L. Guo, Y. Zhang, D. Xie, Z. Hu and Z. Lin, Metabolomics investigation reveals that 8-C *N*-ethyl-2-pyrrolidinone-substituted flavan-3-ols are potential marker compounds of stored white teas, *J. Agric. Food Chem.*, 2018, **66**, 7209–7218.

26 W. Dai, N. Lou, D. Xie, Z. Hu, H. Song, M. Lu, D. Shang, W. Wu, J. Peng, P. Yin and Z. Lin, *N*-ethyl-2-pyrrolidinone-substituted flavan-3-ols with anti-inflammatory activity in lipopolysaccharide-stimulated macrophages are storage-related marker compounds for green tea, *J. Agric. Food Chem.*, 2020, **68**, 12164–12172.

27 D. Xie, W. Dai, M. Lu, J. Tan, Y. Zhang, M. Chen and Z. Lin, Nontargeted metabolomics predicts the storage duration of white teas with 8-C *N*-ethyl-2-pyrrolidinone-substituted flavan-3-ols as marker compounds, *Food Res. Int.*, 2019, **125**, 108635.

28 P. Xu, L. Chen and Y. F. Wang, Effect of storage time on antioxidant activity and inhibition on α-Amylase and α-Glucosidase of white tea, *Food Sci Nutr*, 2019, **7**, 636–644.

29 J. Peng, W. Dai, M. Lu, Y. Yan, Y. Zhang, D. Chen, W. Wu, J. Gao, M. Dong and Z. Lin, New insights into the influences of baking and storage on the nonvolatile compounds in oolong tea: A nontargeted and targeted metabolomics study, *Food Chem.*, 2022, **375**, 131872.

30 A. B. Nair and S. Jacob, A simple practice guide for dose conversion between animals and human, *J. Basic Clin. Pharm.*, 2016, **7**, 27–31.

31 L. Huang, J. P. Zheng, G. J. Sun, H. B. Yang, X. J. Sun, X. W. Yao, A. Z. Lin and H. T. Liu, 5-Aminosalicylic acid ameliorates dextran sulfate sodium-induced colitis in mice by modulating gut microbiota and bile acid metabolism, *Cell. Mol. Life Sci.*, 2022, **79**, 460.

32 H. Lin, Y. P. An, H. R. Tang and Y. L. Wang, Alterations of bile acids and gut microbiota in obesity induced by high fat diet in rat model, *J. Agric. Food Chem.*, 2019, **67**, 3624–3632.

33 C. Yang, Z. Hu, M. Lu, P. Li, J. Tan, M. Chen, H. Lv, Y. Zhu, Y. Zhang, L. Guo, Q. Peng, W. Dai and Z. Lin, Application of metabolomics profiling in the analysis of metabolites and taste quality in different subtypes of white tea, *Food Res. Int.*, 2018, **106**, 909–919.

34 H. Lv, Q. Zhong, Z. Lin, L. Wang, J. Tan and L. Guo, Aroma characterisation of Pu-erh tea using headspace-solid phase microextraction combined with GC/MS and GC–olfactometry, *Food Chem.*, 2012, **130**, 1074–1081.

35 Y. Oritani, Y. Setoguchi, R. Ito, H. Maruki-Uchida, T. Ichiyanagi and T. Ito, Comparison of (−)-epigallocatechin-3-*O*-gallate (EGCG) and *O*-methyl egcg bioavailability in rats, *Biol. Pharm. Bull.*, 2013, **36**, 1577–1582.

36 M. Zhang, X. Zhang, C.-T. Ho and Q. Huang, Chemistry and health effect of tea polyphenol (−)-Epigallocatechin 3-*O*,-(3-*O*-Methyl)gallate, *J. Agric. Food Chem.*, 2019, **67**, 5374–5378.

37 R. H. Mills, P. S. Dulai, Y. Vázquez-Baeza, C. Sauceda, N. Daniel, R. R. Gerner, L. E. Batachari, M. Malfavon, Q. Zhu, K. Weldon, G. Humphrey, M. Carrillo-Terrazas, L. D. Goldasich, M. Bryant, M. Raffatellu, R. A. Quinn, A. T. Gewirtz, B. Chassaing, H. Chu, W. J. Sandborn, P. C. Dorrestein, R. Knight and D. J. Gonzalez, Multi-omics analyses of the ulcerative colitis gut microbiome link *Bacteroides vulgatus* proteases with disease severity, *Nat. Microbiol.*, 2022, **7**, 262–276.

38 Y. X. Zhang, X. Y. Feng, H. Y. Lin, X. Chen, P. M. He, Y. F. Wang and Q. Chu, Tieguanyin extracts ameliorated DSS-induced mouse colitis by suppressing inflammation and regulating intestinal microbiota, *Food Funct.*, 2022, **13**, 13040–13051.

39 G. Chen, M. Wang, Z. Zeng, M. Xie, W. Xu, Y. Peng, W. Zhou, Y. Sun, X. Zeng and Z. Liu, Fuzhuan brick tea polysaccharides serve as a promising candidate for remodeling the gut microbiota from colitis subjects in vitro: Fermentation characteristic and anti-inflammatory activity, *Food Chem.*, 2022, **391**, 133203.

40 L. E. Davey, P. N. Malkus, M. Villa, L. Dolat, Z. C. Holmes, J. Letourneau, E. Ansaldo, L. A. David, G. M. Barton and R. H. Valdivia, A genetic system for *Akkermansia muciniphila* reveals a role for mucin foraging in gut colonization and host sterol biosynthesis gene expression, *Nat. Microbiol.*, 2023, **8**, 1450–1467.

41 A. Bartoszek, E. V. Moo, A. Binienda, A. Fabisiak, J. B. Krajewska, P. Mosińska, K. Niewinna, A. Tarasiuk, K. Martemyanov, M. Salaga and J. Fichna, Free Fatty Acid Receptors as new potential therapeutic target in inflammatory bowel diseases, *Pharmacol. Res.*, 2020, **152**, 104604.

42 G. Chen, X. Ran, B. Li, Y. Li, D. He, B. Huang, S. Fu, J. Liu and W. Wang, Sodium butyrate inhibits inflammation and maintains epithelium barrier integrity in a TNBS-induced inflammatory bowel disease mice model, *EBioMedicine*, 2018, **30**, 317–325.

43 Y. Liu, X. Wang and C.-A. A. Hu, Therapeutic potential of amino acids in inflammatory bowel disease, *Nutrients*, 2017, **9**, 920.

44 S. Vidal-Lletjós, M. Beaumont, D. Tomé, R. Benamouzig, F. Blachier and A. Lan, Dietary protein and amino acid supplementation in inflammatory bowel disease course: What impact on the colonic mucosa?, *Nutrients*, 2017, **9**, 310.

45 W. Ren, J. Yin, M. Wu, G. Liu, G. Yang, Y. Xion, D. Su, L. Wu, T. Li, S. Chen, J. Duan, Y. Yin and G. Wu, Serum amino acids profile and the beneficial effects of L-arginine or L-glutamine supplementation in dextran sulfate sodium colitis, *PLoS One*, 2014, **9**, e88335.

46 M. Faure, C. Mettraux, D. Moennoz, J. P. Godin, J. Vuichoud, F. Rochat, D. Breuillé, C. Obled and I. Corthésy-Theulaz, Specific amino acids increase mucin synthesis and microbiota in dextran sulfate sodium-treated rats, *J. Nutr.*, 2006, **136**, 1558–1564.

47 T. Li, J. Zhang, S. Fei, S. Zhu, J. Zhu, X. Qiao and Z. Liu, Glutamate microinjection into the hypothalamic paraventricular nucleus attenuates ulcerative colitis in rats, *Acta Pharmacol. Sin.*, 2014, **35**, 185–194.

48 D. V. Guzior and R. A. Quinn, Review: microbial transformations of human bile acids, *Microbiome*, 2021, **9**, 140.

49 S. Fiorucci, A. Carino, M. Baldoni, L. Santucci, E. Costanzi, L. Graziosi, E. Distrutti and M. Biagioli, Bile acid signaling in inflammatory bowel diseases, *Dig. Dis. Sci.*, 2021, **66**, 674–693.

50 J. P. Thomas, D. Modos, S. M. Rushbrook, N. Powell and T. Korcsmaros, The Emerging role of bile acids in the pathogenesis of inflammatory bowel disease, *Front. Immunol.*, 2022, **13**, 829525.

51 S. Hang, D. Paik, L. Yao, E. Kim, J. Trinath, J. Lu, S. Ha, B. N. Nelson, S. P. Kelly, L. Wu, Y. Zheng, R. S. Longman, F. Rastinejad, A. S. Devlin, M. R. Krout, M. A. Fischbach, D. R. Littman and J. R. Huh, Bile acid metabolites control TH17 and Treg cell differentiation, *Nature*, 2019, **576**, 143–148.

52 Z. Zhang, H. Zhang, T. Chen, L. Shi, D. Wang and D. Tang, Regulatory role of short-chain fatty acids in inflammatory bowel disease, *Cell Commun. Signaling*, 2022, **20**, 64.

53 M. A. Bromke and M. Krzystek-Korpacka, Bile acid signaling in inflammatory bowel disease, *Int. J. Mol. Sci.*, 2021, **22**, 9096.

54 S. Cao, X. Meng, Y. Li, L. Sun, L. Jiang, H. Xuan and X. Chen, Bile acids elevated in chronic periaortitis could activate farnesoid-X-receptor to suppress IL-6 production by macrophages, *Front. Immunol.*, 2021, **12**, 632864.

55 J. Hu, C. Wang, X. Huang, S. Yi, S. Pan, Y. Zhang, G. Yuan, Q. Cao, X. Ye and H. Li, Gut microbiota-mediated secondary bile acids regulate dendritic cells to attenuate autoimmune uveitis through TGR5 signaling, *Cell Rep.*, 2021, **36**, 109726.

56 X. Song, X. Sun, S. F. Oh, M. Wu, Y. Zhang, W. Zheng, N. Geva-Zatorsky, R. Jupp, D. Mathis, C. Benoist and D. L. Kasper, Microbial bile acid metabolites modulate gut RORγ(+) regulatory T cell homeostasis, *Nature*, 2020, **577**, 410–415.